

Dynamic structure factor for a ferromagnet in the scaling region to first order in $\epsilon = 6 - d$

Michael J. Nolan and Gene F. Mazenko*

Department of Physics and the James Franck Institute, The University of Chicago, Chicago, Illinois 60637

(Received 8 January 1976)

The dynamic structure factor for a model ferromagnet is calculated to order $\epsilon = 6 - d$ for $T \geq T_c$. The dynamic shape function is extracted from the structure factor and plotted for various values of ϵ and $x = k\xi$, where ξ is the correlation length and k the wave number. In the vicinity of T_c and for $\epsilon \gtrsim 0.95$ peaks appear which are characteristic of sloppy spin-wave modes.

Ma and Mazenko¹ (MM) have previously discussed the critical dynamics of a model ferromagnet. The order parameter in their model is the spin density.

$$\vec{S}(\vec{x}, t) = L^{-d/2} \sum_{\kappa\Lambda} \vec{S}_\kappa(t) e^{i\vec{\kappa}\cdot\vec{x}}, \quad (1)$$

which is a three-component vector field. L^d is the volume of the d -dimensional system, and Λ is a wave number cutoff. \vec{S} obeys the equation of motion

$$\frac{\partial \vec{S}}{\partial t} = \lambda \vec{S} \times \vec{H} - \Gamma \nabla^2 \vec{H} + \vec{\xi}, \quad (2)$$

where $\vec{H}(x, t)$ is the local magnetic field; λ and Γ are constants, and $\xi(x, t)$ is a Gaussian random noise. The local magnetic field \vec{H} is derivable from a Ginzburg-Landau free energy $F[\vec{S}]$ and is the sum of an external applied field \vec{h} and the field generated by the spins:

$$\vec{H}(\vec{x}, t) = \vec{h}(\vec{x}, t) - \frac{\delta F[\vec{S}]}{\delta \vec{S}(\vec{x}, t)}, \quad (3)$$

$$F[\vec{S}] = \frac{1}{2} \int d^d x [(\nabla \vec{S})^2 + r_0 \vec{S}^2 + \frac{1}{2} u (\vec{S}^2)^2], \quad (4)$$

where $r_0 = a(T - T_c)$ and a and u are positive constants.

These equations of motion are specified by the parameter set

$$\mu = (\bar{\lambda}, r_0; u, h), \quad \bar{\lambda} \equiv \lambda/\Gamma. \quad (5)$$

By using renormalization-group (RNG) techniques, MM have determined that this model obeys dynamic scaling to $O(\epsilon)$ and have furthermore found a nontrivial fixed-point structure for the parameter set [Eq. (5)]. Using these fixed-point results one can set up a perturbation-theory calculation in $\epsilon = 6 - d$ valid in the scaling region. This perturbation theory is developed in terms of the response function $G(k, \omega)$ defined by

$$\langle S_\alpha^\alpha(\omega) \rangle = G(k, \omega) h_\alpha^\alpha(\omega) + O(h^2), \quad (6)$$

where α is the vector component index. The cor-

relation function $C(k, \omega)$,

$$\langle S_\alpha^\alpha(\omega) S_{\alpha'}^\beta(\omega') \rangle \equiv 2\pi C(k, \omega) \delta_{\alpha, \beta} \delta_{k, -k'} \delta(\omega + \omega'), \quad (7)$$

can be calculated from the response function using the classical fluctuation dissipation theorem

$$C(k, \omega) = (2/\omega) \text{Im} G(k, \omega). \quad (8)$$

It is convenient to write the response function in the form

$$G^{-1}(k, \omega) = -[i\omega/k^2 \Gamma(k, \omega)] + \chi^{-1}(k), \quad (9)$$

where $\Gamma(k, \omega)$ is called the generalized transport coefficient and $\chi(k)$ is the static susceptibility:

$$\chi(k) = \int \frac{d\omega}{2\pi} C(k, \omega). \quad (10)$$

The static susceptibility remains of the Ornstein-Zernicke form to $O(\epsilon)$

$$\chi^{-1}(k) = k^2 + \xi^{-2}, \quad (11)$$

where ξ is the correlation length.

The result of MM for the generalized transport coefficient $\Gamma(k, \omega)$ to $O(\epsilon)$ for $T \geq T_c$ is given by [see Eqs. (5.6)–(5.8) in MM]:

$$\Gamma(k, \omega) = \Gamma(1 + Q(k, \omega)), \quad (12)$$

where

$$Q(k, \omega) = \frac{\bar{\lambda}^{*2}}{k^2} \int \frac{d^6 q}{(2\pi)^6} \frac{[(k-q)^2 - q^2]^2 \chi(q) \chi(k-q)}{D(k, q, \omega)}, \quad (13)$$

$$D(k, q, \omega) = -(i\omega/\Gamma) + q^2 \chi^{-1}(q) + (q-k)^2 \chi^{-1}(q-k). \quad (13a)$$

$\bar{\lambda}^*$ is the fixed-point value of $\bar{\lambda}$ determined by RNG to be

$$\bar{\lambda}^{*2} = 96\pi^3 \epsilon, \quad (14)$$

Once the integral [Eq. (13)] has been evaluated, it is a straightforward matter to extract the correlation function, and, consequently, the shape function $f_x(\nu)$ defined by

$$C(k, \omega) = [\chi(k)/\omega(k)]f_x(\nu), \quad (15)$$

where $x = k\xi$, $\nu = \omega/\omega(k)$, and $\omega(k)$ is the characteristic frequency defined below.

Recent similar calculations by Freedman and Mazenko (FM)² for the antiferromagnet structure factor have revealed peaks in f_x^N at and above T_N where T_N is the Néel temperature. These peaks resemble those observed in the isotropic antiferromagnet RbMnF₃ by neutron scattering.³ We were therefore encouraged to carry out a more thorough analysis of the ferromagnet case to see

if it also would show peaks in the shape function.

All the integrals in Eq. (13), except for one, which was subsequently evaluated on the computer, have been performed analytically. In this analysis we have extracted all logarithmic divergences analytically. The result for the generalized transport coefficient is

$$\Gamma(k, \omega) = \Gamma\left[1 + \frac{1}{2}\epsilon \ln \Lambda \xi + \frac{1}{2}\epsilon \ln 2 + \frac{1}{4}\epsilon \Delta(x, \nu) + \frac{1}{16}\epsilon I(x, \nu)\right], \quad (16)$$

where $\Delta(x, \nu)$ is given by

$$\begin{aligned} \Delta(x, \nu) = & \left(\ln \frac{1}{x^2}\right) \left(1 + \frac{3(t+3)^2}{8ivtx^2} + \frac{4(t+3)^3}{(8ivt)^2x^4} - \frac{(1+\frac{1}{2}x^2+s)^3}{2s(1-s)^2}\right) + (\ln 4) \left(\frac{3(t+3)^2}{8ivtx^2} + \frac{4(t+3)^3}{(8ivt)^2x^4} - \frac{(1+\frac{1}{2}x^2+s)^3}{2s(1-s)^2}\right) \\ & + \left[\ln \left(\frac{t+3}{4}\right)\right] \left(\frac{3(t+3)^2}{8ivtx^2} + \frac{4(t+3)^3}{(8ivt)^2x^4}\right) + \frac{(t+3)^2}{8ivtx^2} - \frac{(1+\frac{1}{2}x^2+s)^3 \ln(\frac{1}{2} + \frac{1}{4}x^2 + \frac{1}{2}s)}{2s(1-s)^2} \\ & + \frac{(1+\frac{1}{2}x^2-s)^3}{2s(1-s)^2} \ln \left[\frac{4}{x^2} \left(\frac{1}{2} + \frac{x^2}{4} - \frac{s}{2}\right)\right] \end{aligned} \quad (17)$$

with

$$s = (1 + 2ivtx^2)^{1/2}, \quad (18a)$$

$$t = 1 + x^2, \quad (18b)$$

$$\nu = \omega/\Gamma k^4(1 + x^{-2}). \quad (18c)$$

$I(x, \nu)$ is given by

$$\begin{aligned} I(x, \nu) = & \int_{\beta}^{\infty} dy \left(y(7-\beta) - 6\beta - 2iv(\beta+3) + y(y^2 - 4y + 4\beta)^{3/2} \right. \\ & \left. - \frac{[y^2 + y(5-\beta) - 4\beta - 2iv(\beta+3)]^{3/2} [y^2 - y(\beta-1) - 2iv(\beta+3)]^{1/2}}{2y^2 - y(\beta-1) - 2iv(\beta+3)} - \frac{4(y-\beta)^3}{y^2[y^2 - y(\beta-1) - 2iv(\beta+3)]} \right), \end{aligned} \quad (19)$$

where

$$\beta = 1 + 4x^{-2}. \quad (19a)$$

We have evaluated $I(x, \nu)$ numerically. Following an elementary exponentiation we may rewrite Eq. (16), correct to $O(\epsilon)$, as

$$\Gamma(k, \omega) = \Gamma(\Lambda \xi)^{\epsilon/2} \left[1 + \frac{1}{2}\epsilon \ln 2 + \frac{1}{4}\epsilon \Delta(x, \nu) + \frac{1}{16}\epsilon I(x, \nu) \right]. \quad (20)$$

This result may be used to calculate the renormalized physical transport coefficient⁴ $\bar{\Gamma}$:

$$\bar{\Gamma} = \lim_{\substack{\omega \rightarrow 0 \\ k \rightarrow 0}} \Gamma(k, \omega) = \Gamma(\Lambda \xi)^{\epsilon/2} (1 - \frac{3}{8}\epsilon). \quad (21)$$

We see from Eq. (21) that the transport coefficient diverges as $\xi^{\epsilon/2}$ as $T \rightarrow T_c$. We take $\bar{\Gamma}$ to be a number fixed by experiment. We can now rewrite

Eq. (20) to $O(\epsilon)$ as

$$\Gamma(k, \omega) = \bar{\Gamma} \left[1 + \frac{3}{8}\epsilon + \frac{1}{2}\epsilon \ln 2 + \frac{1}{4}\epsilon \Delta(x, \nu) + \frac{1}{16}\epsilon I(x, \nu) \right]. \quad (22)$$

By our choice of renormalization, Eq. (22) should accurately give the behavior of $\Gamma(k, \omega)$ for small x and ν . In order to properly treat the large x and ν behavior, certain exponentiations are necessary so that the results are in agreement with the scaling predictions of the RNG. That is, $\Gamma(k, \omega)$ must obey the relation²

$$\Gamma(k, \omega, \xi^{-1}) = b^{-\epsilon+4-\eta} \Gamma(bk, b^\epsilon \omega, b \xi^{-1}),$$

where z and η are exponents to be determined. The static RNG determines η to be identically zero for $d > 4$, and zero to $O(\epsilon)$ for $d \leq 4$. The exponentiation procedure used here follows the guidelines of FM.

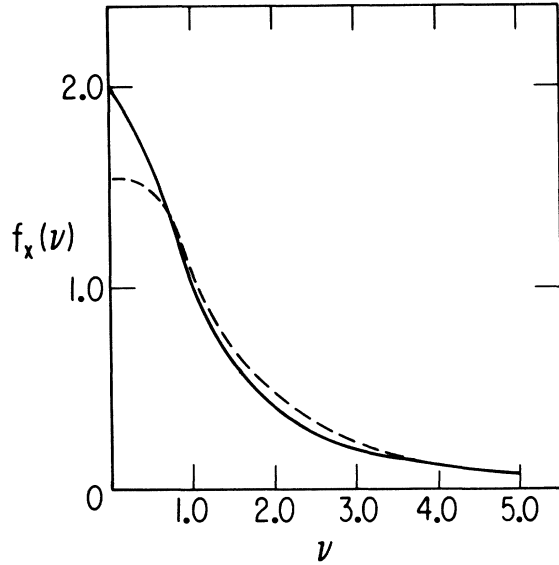


FIG. 1. Shape function plotted vs ν for $\epsilon = 0.0$, x arbitrary, (solid line) and for $\epsilon = 1.0$, $x = \infty$ (dashed line).

Note that our case is slightly special since the ν 's always occur with a factor of x^2 :

$$\Gamma(k, \omega) = \Gamma(x^2, i\nu x^2). \quad (23)$$

In order to carry out the appropriate exponentiations we need to separate out the logarithmic terms in $\Gamma(k, \omega)$ governing the various large and small x, ν limits. We have found that the quantity

$$\Gamma_L(k, \omega) = \tilde{\Gamma}(1 - \frac{1}{4}\epsilon f(x, \nu)), \quad (24)$$

$$f(x, \nu) = \ln(1 + x^2) + \frac{1}{2} \ln\left(1 - \frac{8i\nu x^2}{1 + x^2}\right), \quad (24a)$$

has the property of giving correctly all small and large x, ν limits of $\Gamma(k, \omega)$.⁵ We may then write

$$\Gamma(k, \omega) = \tilde{\Gamma}\left[1 + \frac{3}{8}\epsilon + \frac{1}{2}\epsilon \ln 2 + \frac{1}{16}\epsilon I(x, \nu) + \frac{1}{4}\epsilon \Delta(x, \nu) + \frac{1}{4}\epsilon f(x, \nu) - \frac{1}{4}\epsilon f(x, \nu)\right]. \quad (25)$$

It is now a simple matter to exponentiate the logarithms in $1 - \frac{1}{4}\epsilon f(x, \nu)$ and rewrite Eq. (24) in a form consistent with the RNG scaling predictions to $O(\epsilon)$:

$$\Gamma(k, \omega) = \tilde{\Gamma}(1 + x^2)^{-\epsilon/4} W(x, \nu) \quad (26)$$

$$W(x, \nu) = \left(1 - \frac{8i\nu x^2}{1 + x^2}\right)^{-\epsilon/8} \times \left[1 + \frac{1}{2}\epsilon \ln 2 + \frac{3}{8}\epsilon + \frac{1}{4}\epsilon \Delta(x, \nu) + \frac{1}{16}\epsilon I(x, \nu) + \frac{1}{4}\epsilon \ln(1 + x^2) + \frac{1}{8}\epsilon \ln\left(1 - \frac{8i\nu x^2}{1 + x^2}\right)\right]. \quad (26a)$$

In order to extract the shape function, it is

necessary to define a characteristic frequency. We follow FM and choose the characteristic frequency, $\omega(k)$, in terms of the ν -independent factors in $\Gamma(k, \omega)k^2$ times the inverse static susceptibility

$$\begin{aligned} \omega(k) &= k^2 \tilde{\Gamma}(1 + x^2)^{-\epsilon/4} \chi^{-1}(k) \\ &= k^{4-\epsilon/2} (\tilde{\Gamma}/\xi^{\epsilon/2}) (1 + x^2)^{1-\epsilon/4}. \end{aligned}$$

Then as $x \rightarrow 0$

$$\omega(k) = k^2 \xi^{-2} \tilde{\Gamma},$$

while at T_c

$$\omega(k) = k^{4-\epsilon/2} (\tilde{\Gamma}/\xi^{\epsilon/2}).$$

This choice of $\omega(k)$ is consistent with the dynamic scaling form $\omega(k) = k^z f(x)$ with $z = 4 - \frac{1}{2}\epsilon$. The natural frequency variable is then

$$\nu \equiv \frac{\omega}{\omega(k)} = \frac{\omega}{k^{4-\epsilon/2} (\tilde{\Gamma}/\xi^{\epsilon/2}) (1 + x^2)^{1-\epsilon/4}}. \quad (27)$$

Since we work to $O(\epsilon)$, we can consistently replace the ν 's in Eq. (17) given by Eq. (18c) with the ν given by Eq. (27).

Taking Eq. (15) together with Eqs. (26) and (27), we find that the shape function is given by

$$f_x(\nu) = (2/\nu) \text{Im}(1 - i\nu/W(x, \nu))^{-1}. \quad (28)$$

with $W(x, \nu)$ given in Eq. (26a).

$f_x(\nu)$ is plotted in Figs. 1–4 for various values of x and ϵ . Its behavior may be summarized as follows.

- For $\epsilon \ll 1$, $f_x(\nu)$ is a Lorentzian centered about $\nu = 0$ for all values of x .
- For $x \ll 1$, $f_x(\nu)$ is a Lorentzian for all values of ϵ .
- For $x \gg 1$, fluctuation induced peaks start

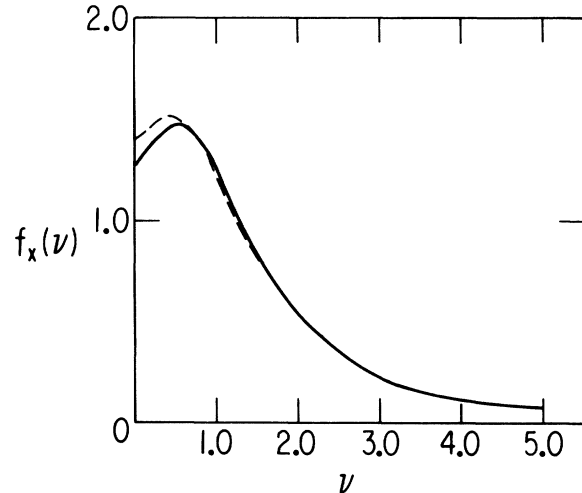


FIG. 2. Shape function plotted vs ν for $\epsilon = 2.0$, $x = \infty$, (solid line) and for $\epsilon = 2.0$, $x = 2.5$ (dashed line).

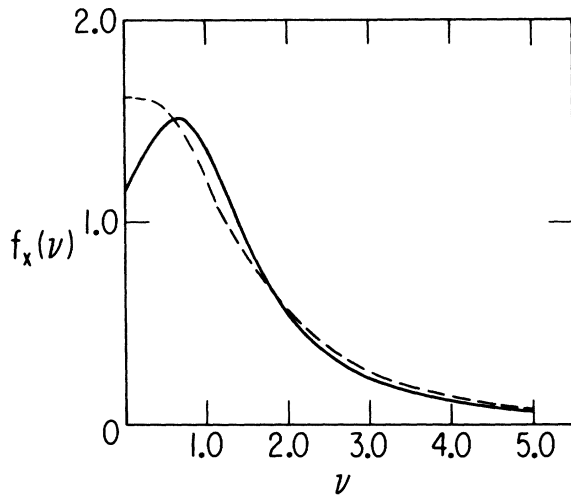


FIG. 3. Shape function plotted vs ν for $\epsilon = 2.5$, $x = \infty$ (solid line) and for $\epsilon = 2.5$, $x = 1.0$ (dashed line).

appearing when $\epsilon \approx 0.95$. As ϵ increases, these peaks steadily become more pronounced as can be characterized by the increasing ratio $r = f_x(\nu_0)/f_x(0)$, where ν_0 is the location of the peak. (See Fig. 5.)

(d). For a fixed value of $\epsilon \geq 0.95$, the peaks first appear at a value of x which is ϵ dependent. The peaks initially appear near $\nu = 0$ and move steadily outward for increasing x until saturation occurs and the peak location remains constant. The value of x where saturation occurs is also ϵ dependent. As the peaks move outward from the origin with increasing x , they become more pronounced (r increases) until again saturation occurs at some ϵ -dependent x .

Wegner has performed a calculation on both the isotropic ferromagnet⁶ and antiferromag-

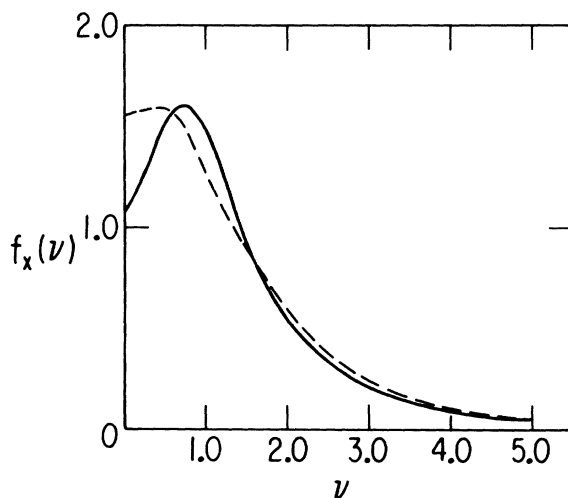


FIG. 4. Shape function plotted vs ν for $\epsilon = 3.0$, $x = \infty$ (solid line) and for $\epsilon = 3.0$, $x = 1.0$ (dashed line).

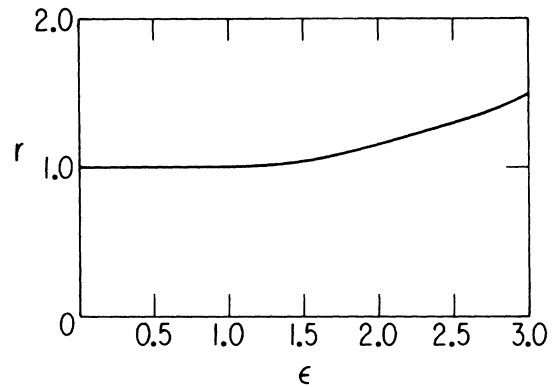


FIG. 5. Ratio $r = f_x(\nu_0)/f_x(0)$, where ν_0 is the peak location, is plotted vs ϵ for $x = \infty$.

net.⁷ Beginning with the microscopic Hamiltonian and utilizing mode-coupling techniques, he derives implicit fourfold integral equations for the self-energy. These equations are subsequently solved self-consistently on a computer. His results for the antiferromagnet are in qualitative agreement with those of FM, while his results for the ferromagnet differ substantially from ours in that no peaks are seen to occur in the shape function.

There are, however, difficulties with the approach Wegner has used. Only the "simplest" contributing diagrams to the self-energy are retained. This mode-coupling approach is then hindered by the lack of a small parameter, and there is no guarantee that the more complex diagram will not significantly alter the results.

It is true that mode-coupling calculations give the correct exponents which characterize the divergent transport coefficients, but there is no perturbative control over the coefficients of these divergences. It is these coefficients which will be important in calculating the shape functions.

These difficulties are avoided with a RNG approach. One of the main contributions of the RNG has been to show how to develop a systematic procedure for carrying out mode-coupling calculations. The introduction of the small parameter ϵ allows one to perform a consistent perturbation expansion.

The RNG also offers some insight into a comparison of the ferromagnet and antiferromagnet results. According to the RNG, the fluctuations for the ferromagnet are stronger than for the antiferromagnet as evidenced by the need to work near six rather than four dimensions. Consequently, the fluctuations of the neglected more-complex diagrams in an expansion like that of Wegner's render the calculation less reliable for ferromagnets than for antiferromagnets.

There is, of course, no reason why our results should be believed when we extrapolate to $\epsilon = 3$. We have included this case in our calculations because our results remain physically reasonable and indicate how the strength of the fluctuations grow as we increase ϵ . These results for the ferromagnet are qualitatively different from the results of FM for the antiferromagnet in one respect. At T_c the ferromagnet peak is considerably sharper than that of the antiferromagnet. In three dimensions at T_c we have $\gamma \approx 1.5$ for the ferromagnet

in contrast to $\gamma \approx 1.15$ for the antiferromagnet. However, the ferromagnet peaks have not been observed experimentally. We have compared our results to available experimental data on Ni,⁸ and Fe.⁹ For Ni, at a momentum transfer of $k = 0.075 \text{ \AA}^{-1}$, our equations predict that the peak should occur at an energy transfer of $\hbar\omega \approx 0.4 \text{ meV}$. For F_e , with $k = 0.05 \text{ \AA}^{-1}$, the corresponding energy value is $\hbar\omega \approx 0.04 \text{ meV}$. We do not believe these peaks could have been observed by these workers given their experimental resolution.

*Research supported in part by the National Science Foundation and the Louis Block Fund, The University of Chicago.

¹S. Ma and G. Mazenko, Phys. Rev. Lett. **33**, 1383 (1974); Phys. Rev. B **11**, 4077 (1975). We use the notation of these authors.

²R. Freedman and G. Mazenko, Phys. Rev. Lett. **34**, 4077 (1975), and unpublished.

³A. Tucciarone, H. Y. Lau, L. M. Corliss, A. Delapalme, and J. W. Hastings, Phys. Rev. B **4**, 3206 (1971).

⁴The observant reader may note that for $\epsilon > \frac{8}{3}$ it appears that $\tilde{\Gamma}$ becomes negative which is unphysical. This difficulty may be avoided by noting that the factor $\frac{1}{2}\epsilon$ that we exponentiated is arbitrary. Thus, to $O(\epsilon)$ we can write $[(\Lambda/\Lambda')\Lambda']^{\epsilon/2} = (\Lambda')^{\epsilon/2}(1 + \frac{1}{2}\epsilon \ln \Lambda/\Lambda')$, so that $\tilde{\Gamma} = \Gamma(\xi \Lambda')^{\epsilon/2}[1 + \frac{1}{2}\epsilon(\ln \Lambda/\Lambda' - \frac{2}{3})]$. If we pick $\Lambda/\Lambda' = c^R$

such that $R > \frac{3}{4}$, then *positivity* is ensured.

⁵By this we mean the four possible limits: (a) large x , large ν ; (b) small x , small ν ; (c) small x , large νx^2 ; (d) large x , small νx^2 . Note also that to give the proper large ν , small x behavior, we must write the coefficient of ν in the logarithm in the form $\nu x^2/(a+x^2)$. We have determined a by first taking the large ν limit with x arbitrary and then allowing x to become large. The factor a is then found by analyzing terms of $O(i\nu/x^2)$.

⁶F. Wegner, Z. Phys. (Leipz.) **216**, 433 (1968).

⁷F. Wegner, Z. Phys. (Leipz.) **218**, 265 (1969).

⁸V. J. Minkiewicz, M. F. Collins, R. Nathans, and G. Shirane, Phys. Rev. **182**, 624 (1969).

⁹M. F. Collins, V. J. Minkiewicz, R. Nathans, L. Passell, and G. Shirane, Phys. Rev. **179**, 417 (1969).